V European Conference on Computational Fluid Dynamics
ECCOMAS CFD 2010
J. C. F. Pereira and A. Sequeira (Eds)
Lisbon, Portugal, 14–17 June 2010

SIMULATION OF A BUTTON-TYPE SOLID OXIDE FUEL CELL

E. Vakouftsi[1], G. Marnellos[1,2], C. Athanasiou[2], F.A. Coutelieris[3]

[1]Dept. of Mechanical Engineering, University of Western Macedonia
Bakola & Sialvera Sts, 50100 Kozani, Greece

[2]Chemical Process Engineering Research Institute, Centre for Research & Technology
6th km. Charilaou – Thermi Rd., 57001 Thermi, Thessaloniki, Greece

[3]Dept. of Environmental and Natural Resources Management, University of Ioannina
2 G. Seferi St, 30100 Agrinio, Greece, e-mail: fkoutel@cc.uoi.gr

Keywords: fuel cell, button-type, transport processes, modeling, syngas

Abstract. *Fuel cells are electrochemical devices that directly convert the chemical energy of the fuel into electricity, overcoming Carnot limitations. Unlike batteries, fuel cells can generate electricity continuously under fuel supply. Due to the relatively high operating temperature (800-1000 ^{o}C) appearing in Solid Oxide Fuel Cells (SOFCs), electrochemical reaction kinetics are promoted allowing not only the use of low cost catalysts, but promising higher efficiencies by recovering the high quality waste heat in co-generator plants. The button cell geometry is the simplest set up that can be used to study SOFC performance in laboratory scale experiments and thus contribute to their future development. Based on this geometry, in the current work a SOFC was simulated, which consisted of a porous anode and a cathode electrode separated by a dense electrolyte layer. Two different compositions, a hydrogen-rich gas mixture and a biomass derived syngas mixture, were supplied to the anode, while cathode was exposed to atmospheric air of typical composition, thus providing the necessary ions to electrochemically oxidize the hydrogen. Refer to the model, the strongly coupled equations for the flow field, the mass and energy transport as well as the Butler-Volmer equation for charge transport, were taken into consideration. Towards the most accurate simulation, it was assumed that the relevant gases followed the ideal gas law and the electrodes were modeled as isotropic porous media, while the species distributions were mainly governed by the electrochemical reactions taking place at the gas phases and at the interfaces of the porous electrodes. The system of the above mentioned partial differential equations along with the appropriate boundary conditions were numerically integrated by using the commercially available CFD-ACE+ software by ESI Group, which is based on the finite volume method. Complimentary to the polarization curves (I-P-V curves), the velocity field, the temperature spatial profile as well as the species mass fractions distribution were obtained for constant mass flow rate and temperature at the fuel inlet. The numerical approximations showed good agreement with the experimental results provided elsewhere.*

1 INTRODUCTION

Fuel Cells (FCs) seem to be one potential answer to the discovery of new energy production technologies that would utilize current fuels more effectively. In general, FCs offer to the energy policy makers the alternative choice of having energy independence under fully environmental-friendly conditions. At the same time, used autonomously or even be connected in parallel with the electrical grid, they offer stability and energy production with reduced emissions compared to the conventional energy systems [1].

Fuel cells are electrochemical devices that directly convert the chemical energy of the gaseous fuels into electricity, overcoming Carnot limitations. Theoretically, they can reach high efficiencies and unlike batteries, are able to generate continuous electric power supply (DC) when replenished with fuel. Furthermore, fuel cells are very compact units without moving parts, assuring therefore silent operation, fewer materials design constraints and quite large portability. In general, a typical fuel cell consists of a membrane-electrode assembly (MEA) and the gas channels (anode and cathode channel). Atmospheric air flows towards cathode electrode, while the fuel (usually a hydrogen-rich mixture) is introduced to the anode electrode. The formation of steam-water from hydrogen and oxygen and the production of electricity and heat are the outcomes of the whole processes [2].

Among the other types of fuel cells, Solid Oxide Fuel Cells (SOFCs) present considerable advantages due to their high operating temperature, which favors electrochemical reaction kinetics permitting the use of low cost metal catalysts, while it promises higher efficiencies when recovering the high energy waste heat. Furthermore, SOFC operation allows external or even internal reforming reaction to occur, thus fuels such as carbon monoxide and hydrocarbon fuels that are considered as poison to low temperature fuel cells, can be used with minimal fuel processing [3]. However, apart from the benefits mentioned above, there are some drawbacks regarding the materials used caused mainly by the high temperature, such as thermal expansion of the different fuel cell components and stability issues due to mechanical deficiencies and catalyst deactivation that need to be confronted. A lot of effort has been made in fabricating new, cost effective materials with improved physical and electrochemical characteristics which would enhance both SOFC performance and stability [4].

Button cell SOFCs are widely used to experimental procedures and their MEA assemblies could be either circular or planar, having approximately a diameter of 1 to 3 centimeters which corresponds to an area of 10 to 500 square centimeters, respectively. The majority of experiments reported in literature are conducted inside furnace tubes to control the relatively high temperature gradients that might cause material failures. The experimental results usually refer to polarization characteristics and consequently, due to the large number of available data, a lot of simulation studies, found in literature, are validated against these experimental results. Research is mainly focused on the investigation of new material performances and to the acquisition of a deeper insight on the fuel cells behavior by examining the operating cell voltage, the inlet flow rate and the feedstock composition [5, 6].

Under this respect, in the present paper, a mathematical model describing the transport processes occurring in a button-type FC has been developed. The advection/diffusion phenomena coupled with the electrochemical reactions were considered for two different feed-streams: pure hydrogen and syngas composition (a mixture of H_2, H_2O, CO, CO_2 and N_2). The simulations carried out were validated against experimental data obtained by Suwanwarangkul et al. [7].

2 THEORY

2.1 Transport Phenomena

For a typical button cell design, the fundamental transport phenomena occurring are the flow and heat transfer, the mass transport as well as the charge transfer, which are described by the equations of continuity, momentum and species (neutral or charged) conservation equation. Therefore, the velocity field, the temperature profile, the gas composition and the electric potential distribution of the fuel cell can be calculated. Since laminar conditions are usually assumed, the flow can be well described by the Navier-Stokes equations, which for incompressible fluids are given as:

$$\frac{\partial(\underline{u})}{\partial t}+(\underline{u}\cdot\nabla)\underline{u}=-\frac{1}{\rho}\nabla p+\nu\left(\nabla^2\cdot\underline{u}\right) \qquad (1)$$

where $\underline{u}$ is the velocity vector, ρ the density, p the pressure and ν the kinematic viscosity. By neglecting radiation, the energy balance in the system can be written as:

$$\frac{\partial(\rho c_p T)}{\partial t}+(\underline{u}\cdot\nabla)(\rho c_p T)=\left[\nabla\cdot a\nabla(\rho c_p T)\right]-(\rho c_p T)(\nabla\cdot\underline{u})+\dot{Q} \qquad (2)$$

where T is the temperature, c_p is the heat capacity of the mixture, a is the thermal diffusivity coefficient and $\dot{Q}$ is the amount of heat produced/consumed due to reactions. Taking into account the involving reactions, the species mass fractions were obtained by numerically solving the convective diffusion equation:

$$\frac{\partial(\rho x_i)}{\partial t}+\nabla\cdot(\rho\underline{u}x_i)-\nabla\cdot(\rho D_{i,mix}\nabla x_i)+\dot{\omega}=0 \qquad (3)$$

where x_i is the species i mass fraction, $D_{i,mix}$ is its thermal diffusivity coefficient and $\dot{\omega}$ is the non linear term representing the volumetric production/destruction rate of species i due to reactions. This term will be further clarified later.

2.2 Surface reactions-Electrochemistry

The electrochemical reactions are taking place at the interface between catalyst and ionic conductor and the gas phase, the so called three-phase boundary layer (TPB). Precisely, in the present study we presumed that H_2 is electrochemically oxidized at the three phase boundary of the porous anode electrode according to the following reaction [8]:

$$H_2+O^{2-}\rightarrow H_2O+2e^- \qquad (4)$$

while the O^{2-} produced from the surface reaction (oxygen reduction):

$$O_2+4e^-\rightarrow 2O^{2-} \qquad (5)$$

migrated from the porous cathode electrode.

Regarding the charge conservation, in conducting materials, the sum of all current flows should be zero based on elecro-neutrality. Thus, the current conservation equation is:

$$\nabla \cdot \underline{i} = 0 \qquad (6)$$

where $\underline{i}$ is the current density vector. However, based on the analysis of Newman & Tabias [9], the charge transport consists of electronic and ionic phase transports. During electrochemical reactions, electrons are either transferred from the pores (ionic phase) to the solid region (electronic phase) or vice versa, i.e. the electron transfer is expressed as the transfer current, j_T, where

$$-\nabla \cdot \underline{i_F} = \nabla \cdot \underline{i_S} = j_T \qquad (7)$$

where $\underline{i_F}$ is the current density vector flowing through the pores (ionic phase) and $\underline{i_S}$ is the current density vector flowing through the solid parts of the porous medium (electronic phase). By applying the Ohm law, the transfer current yields:

$$\nabla \cdot \left(\sigma_F \nabla \varphi_F\right) = -\nabla \cdot \left(\sigma_S \nabla \varphi_S\right) = j_T \qquad (8)$$

where σ_F and σ_S are the ionic phase conductivity and the solid phase conductivity, respectively, while φ_F and φ_S are the ionic potential of the fluid and of the electric potential of the solid, respectively. For the non-conducting electrolyte the above equation becomes:

$$\nabla \cdot \left(\sigma_F \nabla \varphi_F\right) + \nabla \cdot \left(\sigma_S \nabla \varphi_S\right) = 0 \qquad (9)$$

and the current transfer j_T can be defined through the Butler-Volmer equation as:

$$j_T = \frac{j_0\left(A/V\right)}{\prod_{i=1}^{N}\left[C_{i,ref}\right]^{a_{i_e}}}\left[\exp\left(\frac{a_a F}{RT}\eta\right) - \exp\left(-\frac{a_c F}{RT}\eta\right)\right]\prod_{i=1}^{N}\left[C_i\right]^{a_{i_e}} \qquad (10)$$

where i_e indexes the electrochemical reactions, j_0 is the exchange current density, a_a and a_c are the anodic and cathodic charge transfer coefficients, respectively, determined by the Tafel plots, N is the total number of reacting species, $\left[C_i\right]$ is the near wall molar concentration of the $i-th$ reacting species or expressed in mass fractions is $\left[C_i\right] = \rho \frac{Y_i}{M_i}$, where M_i is the molar weight of the $i-th$ species, $\left[C_{i,ref}\right]$ is the molar concentration at a reference state at inlet and a_k is the concentration exponent. The overpotential, η, can be expressed as the potential difference between the solid phase and the porous phase potential,

$$\eta = \varphi_S - \varphi_F \qquad (11)$$

For the electrochemical reactions, the production/destruction rate is expressed through the current transfer by the relation [10]

$$\dot{\omega} = \left(b_{PR} - b_R\right)\frac{j_T}{F} \qquad (12)$$

where b_{PR} and b_R are the stoichiometric coefficients of the products and reactants, respectively and F is the Faraday constant.

3 SIMULATIONS

The numerical solution for the above mentioned equations was obtained by the commercial package CFD-ACE+, which is based on the finite volume method. In this approach, the solution domain is divided into a number of cells known as control volumes and the governing equations are numerically integrated over each of these computational cells. CFD-ACE+ employs a co-located cell-centered variable arrangement, and the relative equations are written at each cell for the average value of each quantity, given by its value at the cell center. The Conjugate-Gradient-Squared (CGS) algorithm [11] as well as the Algebraic Multi-Grid (AMG) technique [12], are used to numerically solve the linear algebraic system produced by the discretisation of the differential equations. Calculations were performed on a simple PC, equipped with an Intel© Duo Core processor and 2 GB of RAM, using Windows XP© operating system. On average, the calculations took about 6 hours in order to achieve residual values for all the quantities less than 10^{-4}.

3.1 Geometry

For the current study, the geometry of the simulated fuel cell was based on a typical button cell design, presented in detail elsewhere [7]. The SOFC consisted of the MEA assembly i.e. the porous anode and cathode electrodes where the reactions occurred and the dense electrolyte through which oxygen ions migrated to reach anode electrode. The feedstock was introduced to the fuel channel though an external tube and it flowed along the porous anode layer, being electrochemically oxidized, while the air channel was exposed to atmospheric air. Since the cathode was directly exposed to ambient air, no feed channel was required.

The fuel cell was discretized in space by structured grid consisting of 25590 cells, as depicted in Fig. 1. A finer grid consisted of 95910 cells was also tested and the calculations required approximately 15 hours to converge, indicating less than 1 % deviation from the original results.

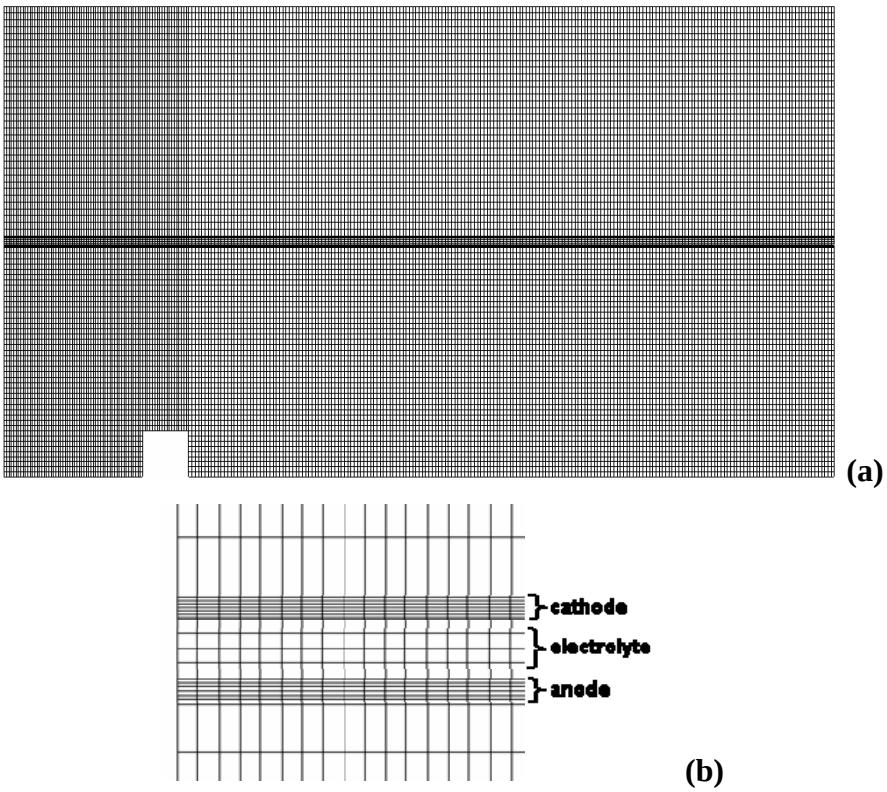

Figure 1: The non-uniform grid for the computational area (a) and a blow-up of the area of interest (b).

3.2 Boundary conditions

Regarding the boundary conditions, the mass flow rates for the anodic mixtures were assumed to be constant and equal to 100 and 180 ml/min, while cathode channel was exposed to ambient air. Fixed pressure of 1 atm was set at the inlets and outlets, as well. Considering no accumulation, zero mass flux was set at the walls and at the outlets. Additionally, all the mixtures were preheated to 1073K before entering the fuel cell, while isothermal conditions of 1073K were set at all the other boundaries to adequately simulate the furnace existence. Finally, constant value of zero potential was set to the anode electrode, while the potential at cathode electrode varied from 0.1 to 0.5 V.

3.3 Parameters

Both electrodes were modeled as isotropic porous media and their physical characteristics are listed in the following Table 1.

	Anode	Electrolyte	Cathode
Porosity [-]	0.40	0.01	0.50
Permeability [-]	10^{-12}	10^{-18}	10^{-12}
Tortuosity [-]	2	2	2
Thermal conductivity [$Wm^{-1}K^{-1}$]	6.23	2.7	9.6
Electronic phase conductivity [$\Omega^{-1}m^{-1}$]	10^{6}	10^{-20}	7700
Ionic phase conductivity [$\Omega^{-1}m^{-1}$]	10	10	10

j_0 [Am^{-3}]	10^{11}	-	10^{10}
a_a [-]	0.7	-	-
a_c [-]	-	-	0.7

Table 1: Porous media properties.

Furthermore, it was assumed that the gases followed the ideal gas law of gases for the calculation of density [kg m^{-3}] and the kinetic theory of gases was used to estimate the viscosity [kg m^{-1} s^{-1}]. The specific heat [J kg^{-1} K^{-1}] derived by fittings to the experimental JANNAF curves and the mass diffusivity (kg m^{-1} s^{-1}) was calculated by a Schmidt number equal to 0.7.

3.4 Assumptions

To achieve the solution, the assumptions made are described below:

- Flow: laminar conditions for compressible fluids, no gravitational effects, Darcy's law for porous regions
- Heat transfer: no radiation
- Mass transport: no accumulation
- Charge transfer: Ohm's law, Butler-Volmer equation
- Feed-stream: In order to investigate the effect of hydrogen content in the feed-stream, two different compositions were considered: pure hydrogen (100% H_2) and typical syngas (20% H_2, 3% H_2O, 20% CO, 14% CO_2 and 43% N_2).
- Atmospheric air: typical composition (21 % mol O_2 and 79 % mol N_2).

4 RESULTS & DISCUSSION

As far as axial and plane symmetry are considered, only a simple part of the actual button cell was considered in the model using two dimensional cylindrical coordinates, as shown in the results presented below.

The velocity field inside the fuel channel is presented in Fig. 2 for the case of syngas supply, when the flow-rate at the inlet of the anode channel is Q_a = 180 ml/min and the cell voltage is V_c = 0.7 V. Obviously, the non-slip condition is fulfilled at the solid walls. It should been underlined that the velocity presents higher values near the inlet, being decreased towards the exit because of the different areas of input and output, which correspond to different velocities. This gradual decrease of the convective regime favors the temperature increase towards the outlet, due to the heat produced by the exothermal electro-oxidation of the fuel over the anode electrode, as it is clearly presented in Fig. 3. Finally, in Fig. 4, the temperature variation along a line in the middle of the anode electrode is presented for the same feed-stream conditions mentioned above, while several cell voltage values are examined. As the exothermic electrochemical oxidation of hydrogen progresses along the anode electrode, the temperature increases towards the exit for every cell voltage, approaching a maximum value in a specific distance from the exit. After this maximum, fuel cell temperature sharply decreases in order for the isothermal condition to be satisfied. Furthermore, it should be mentioned that for lower values of cell voltage the temperature increases, which can be attributed to the increased electrochemical kinetics achieved.

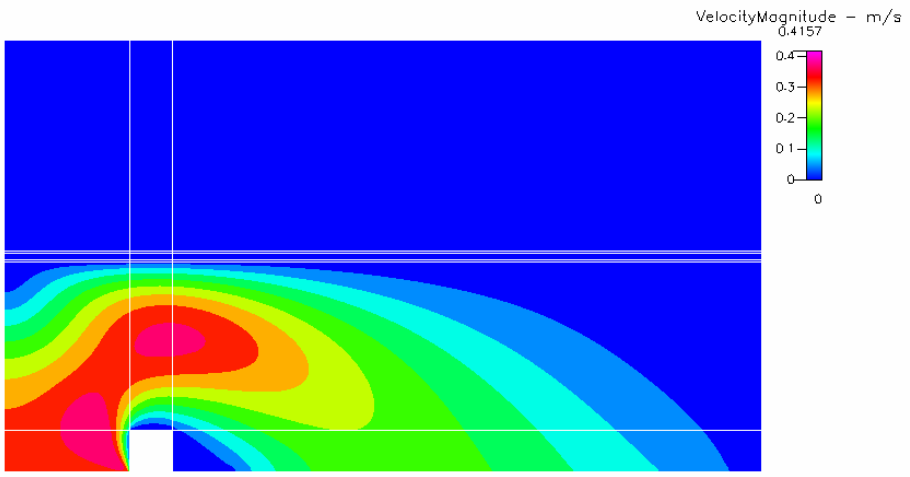

Figure 2: Velocity field for the syngas feeding condition.

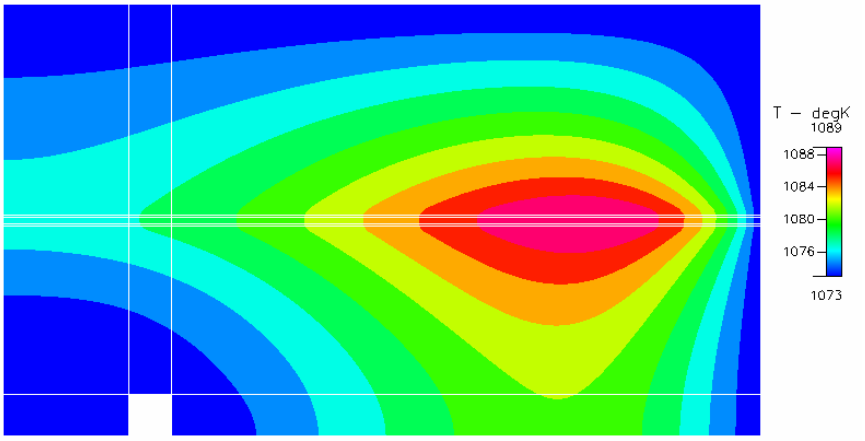

Figure 3: Temperature profile within the syngas-fed fuel cell.

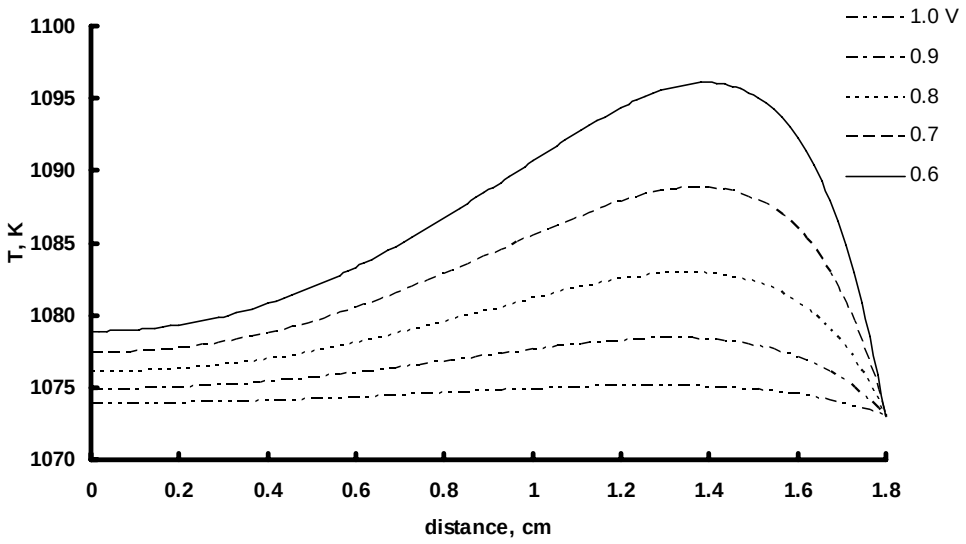

Figure 4: Temperature variation along a line in the middle of the anode electrode for various cell voltages.

The spatial distributions of the involved species at reaction (4) are displayed in the following pictures. More precisely, Fig. 5 depicts the consumption of hydrogen within the fuel cell, while Fig. 6 presents the consequent steam production. It is found that the temperature distribution within the fuel cell follows the species behavior, since the hydrogen is mostly consumed and steam is very much produced in the area where the temperature gets its higher values (towards the wall of the cell). As expected, the rate of hydrogen consumption is quite analogous to that of steam production.

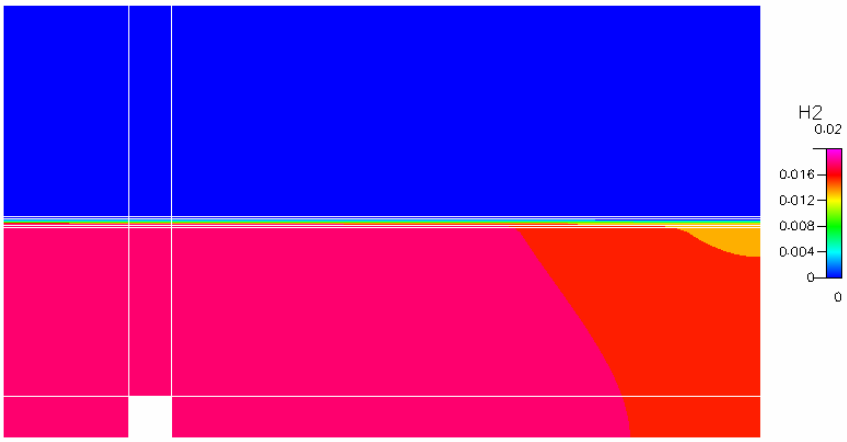

Figure 5: Hydrogen consumption in the button cell.

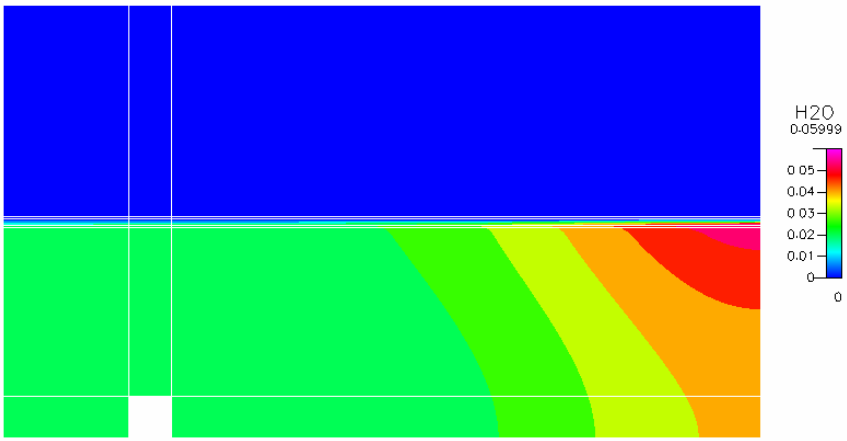

Figure 6: Steam production in the button cell.

The model described in this study is validated against experimental data reported by Suwanwarangkul et al. [7] and the results presented in Fig. 7 depict the relative polarization curves. Fig. 7a shows the results for the case of pure hydrogen feed-stream, while the case of syngas supply for the fuel cell is presented in Fig. 7b. It can be seen that the model shows excellent agreement with the experimental results for both cases. It is also found that, the fuel cell voltage deviates from the open circuit voltage as the produced electrical energy (current density) increases, due to the overpotential losses (activation, ohmic and concentration overpotential).

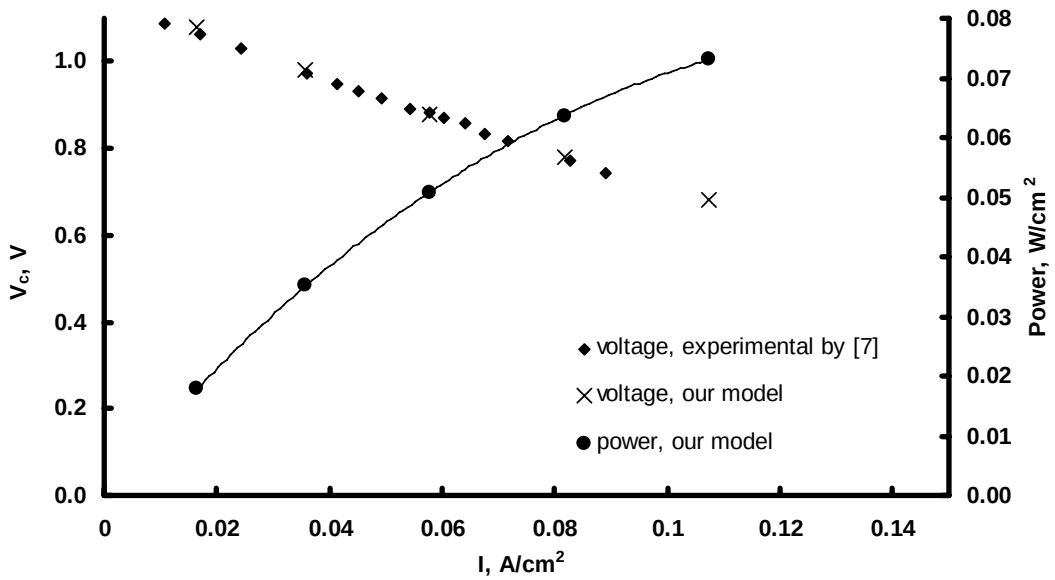

(a)

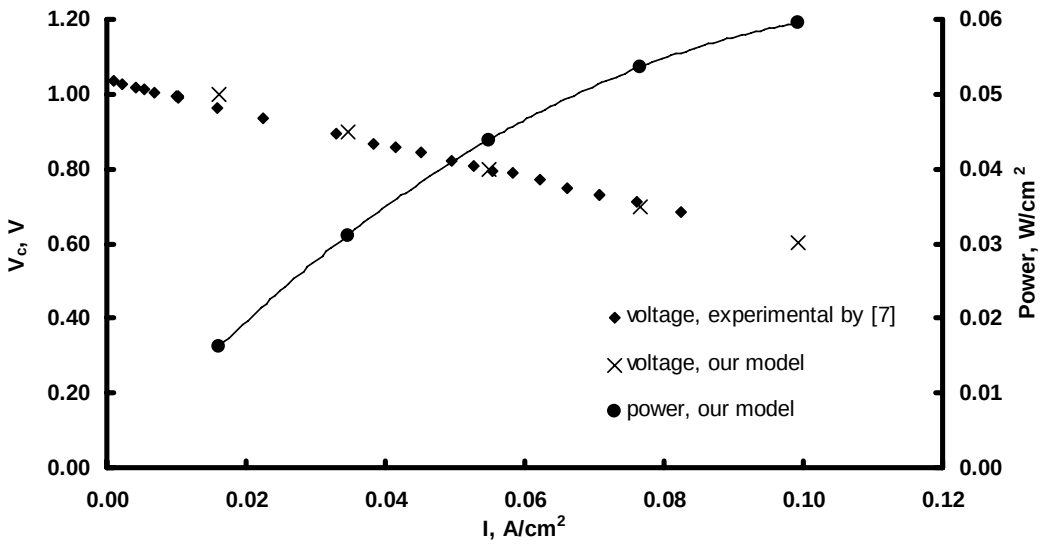

(b)

Figure 7: Polarization curves for the pure hydrogen (a) and syngas (b) feeding conditions.

5 CONCLUSIONS

In the current study the performance of a button-type SOFC was examined and the fundamental transport processes were simulated assuming isothermal conditions at the surroundings of the fuel cell. However, it was found that, regardless the small fuel cell length, there is a significant temperature difference inside the fuel cell and precisely, the temperature was higher at the area close to the exit where the hydrogen oxidation is strong. The increased kinetics due to higher temperature values at the fuel cell reinforce the oxygen ions kinetics and therefore increase the current production. Finally, it could be concluded that the hydrogen fed FC presents improved performance compared to the syngas-fed one, but this difference is less than 10%, indicating the worth of syngas as primary fuel for FC supply.

REFERENCES

[1] J. Larminie and A. Dicks, Fuel cell systems explained. *John Wiley & Sons Ltd*. (2002)

[2] W. Vielstich, A. Lamm and H.A. Gasteiger, Handbook of fuel cells Fundamentals Technology and Applications, *John Wiley & Sons Ltd.* (2003)

[3] F.A. Coutelieris, S. Douvartzides and P. Tsiakaras, The importance of the fuel choice on the efficiency of a solid oxide fuel cell system, *J. Power Sources* **123**, pp. 200 – 205 (2003)

[4] E.V. Tsipis and V.V. Kharton. Electrode materials and reaction mechanisms in solid oxide fuel cells: a brief review II. Electrochemical behavior vs. materials science aspects, *J. Solid State Electr.* **12**, pp. 1367 – 1391 (2008)

[5] I. Zinovik and D. Poulikakos. Modeling the temperature field in the reforming anode of a button-shaped solid oxide fuel cell, *Elecrochem. Acta* **54**, pp. 6234 – 6243 (2009)

[6] G.M. Goldin, H. Zhu, R.J. Kee, D. Bierschenk and S.A. Barnett. Multidimentional flow, thermal, and chemical behaviour in solid-oxide fuel cell button cells, *J. Power Sources* **187**, p. 123 – 135 (2009)

[7] R. Suwanwarangkul, E. Croiset, E. Entchev, S. Charojrochkul, M.D. Pritzker, M.W. Fowler, P.L. Douglas, S. Chewathanakup and H. Mahaudom, Experimental and modelling study of solid oxide fuel cell operating with syngas fuel. *J. Power Sources* **37**, pp. 3323–3341 (1994)

[8] J.-M. Klein,Y. Bultel, S. Georges and M. Pons, Modeling of a SOFC fuelled by methane: From direct internal reforming to gradual internal reforming. *Chem. Eng. Sci.* **62**, pp. 1636-1649 (2007)

[9] J.S. Newman and C.W. Tabias, Theoretical analysis of current distribution in porous electrodes, *J. Electrochem. Soc*. **109,** pp. 1183 – 1191 (1962)

[10] F. Jaouen, G. Lindbergh and G. Sundholm, Investigation of mass-transport limitations in the solid polymer fuel cell cathode, *J. Electrochem. Soc.* **149**, pp. A437-A447 (2002)

[11] Y. Saad, Iterative Methods for Sparse Linear Systems. *PWS* (1996)

[12] R.D. Lonsdale, An algebraic multigrid solver for the Navier-Stokes equations on unstructured meshes. *Int. J. Num. Meth. Heat Fluid Flow*, **3**, pp. 3-14 (1993)